

## Late Quaternary sedimentological and climate changes at Lake Bosumtwi Ghana: New constraints from laminae analysis and radiocarbon age modeling

Timothy M. Shanahan<sup>a,b,\*</sup>, J. Warren Beck<sup>c</sup>, Jonathan T. Overpeck<sup>b,d</sup>, Nicholas P. McKay<sup>b</sup>, Jeffrey S. Pigati<sup>b,e</sup>, John A. Peck<sup>f</sup>, Christopher A. Scholz<sup>g</sup>, Clifford W. Heil Jr.<sup>h</sup>, John King<sup>h</sup>

<sup>a</sup> Jackson School of Geosciences, The University of Texas at Austin, Austin, TX 78713, USA

<sup>b</sup> Department of Geosciences, University of Arizona, Tucson, AZ 85721, USA

<sup>c</sup> Department of Physics, University of Arizona, Tucson, AZ 85721, USA

<sup>d</sup> Institute for the Environment, University of Arizona, Tucson, AZ 85721, USA

<sup>e</sup> United States Geological Survey, Denver, CO 80225, USA

<sup>f</sup> Department of Geology and Environmental Science, University of Akron, Akron, OH 44325, USA

<sup>g</sup> Department of Earth Sciences, Syracuse University, Syracuse, NY 13244, USA

<sup>h</sup> Graduate School of Oceanography, University of Rhode Island, Narragansett, RI 02882, USA

### ARTICLE INFO

#### Article history:

Received 18 April 2012

Received in revised form 26 July 2012

Accepted 1 August 2012

Available online 8 August 2012

#### Keywords:

West Africa  
Paleoclimate  
Lake  
Radiocarbon  
Age model

### ABSTRACT

The Lake Bosumtwi sediment record represents one of the longest and highest-resolution terrestrial records of paleoclimate change available from sub-Saharan Africa. Here we report a new sediment age model framework for the last ~45 cal kyr of sedimentation using a combination of high-resolution radiocarbon dating, Bayesian age-depth modeling and lamination counting. Our results highlight the practical limits of these methods for reducing age model uncertainties and suggest that even with very high sampling densities, radiocarbon uncertainties of at least a few hundred years are unavoidable. Age model uncertainties are smallest during the Holocene (205 yr) and the glacial (360 yr) but are large at the base of the record (1660 yr), due to a combination of decreasing sample density, larger calibration uncertainties and increases in radiocarbon age scatter. For portions of the chronology older than ~35 cal kyr, additional considerations, such as the use of a low-blank graphitization system and more rigorous sample pretreatment were necessary to generate a reliable age depth model because of the incorporation of small amounts of younger carbon. A comparison of radiocarbon age model results and lamination counts over the time interval ~15–30 cal kyr agree with an overall discrepancy of ~10% and display similar changes in sedimentation rate, supporting the annual nature of sediment laminations in the early part of the record. Changes in sedimentation rates reconstructed from the age-depth model indicate that intervals of enhanced sediment delivery occurred at 16–19, 24 and 29–31 cal kyr, broadly synchronous with reconstructed drought episodes elsewhere in northern West Africa and potentially, with changes in Atlantic meridional heat transport during North Atlantic Heinrich events. These data suggest that millennial-scale drought events in the West African monsoon region were latitudinally extensive, reaching within several hundred kilometers of the Guinea coast. This is inconsistent with a simple southward shift in the mean position of the monsoon rainbelt, and requires changes in moisture convergence as a result of either a reduction in the moisture content of the tropical rainbelt, decreased convection, or both.

© 2012 Elsevier B.V. All rights reserved.

### 1. Introduction

The development of robust and accurate age models for sediment records is crucial to the interpretation of sediment proxy-based paleoenvironmental reconstructions as well as for assessing the relative synchrony or asynchrony of reconstructed events. This is particularly true for high-resolution studies, where the frequency of individual events may approach or exceed the uncertainties in the individual

radiometric ages used to develop the sediment chronology. However, the uncertainties, potential biases and complexities inherent in age model development and their influence on the interpretation of high frequency paleoenvironmental changes are often overlooked (e.g., see review in Blaauw, 2010). These problems are particularly challenging with respect to the use of radiocarbon dating because individual <sup>14</sup>C dates cannot be accurately represented by single ages because of plateaus in the calibration curve (Bronk Ramsey, 1998; Reimer et al., 2004; Telford et al., 2004b). This results in non-unique calendar age solutions that are best represented by an irregular distribution of ages. Age modeling of radiocarbon dated sediment records further complicates these issues because of the challenges associated with

\* Corresponding author at: Jackson School of Geosciences, The University of Texas at Austin, Austin, TX 78713, USA. +1 512 232 7051.

E-mail address: [tshanahan@jsg.utexas.edu](mailto:tshanahan@jsg.utexas.edu) (T.M. Shanahan).

incorporating these dating errors into a continuous age-depth model (Telford et al., 2004a). In recent years, a number of new chronostratigraphic approaches have been developed to tackle these issues (Blaauw and Christen, 2005; Heegaard et al., 2005; Bronk Ramsey, 2008; Blaauw, 2010). Some use traditional age-depth modeling techniques, but attempt to provide estimates of uncertainties in interpolated ages using the calibrated radiocarbon age distributions (Blaauw, 2010). Another approach is to use Bayesian modeling to take advantage of the sequential nature of radiocarbon dates in calibration and age model development (Buck et al., 1999). In the present study, we compare these approaches for the development of a new radiocarbon chronology for Lake Bosumtwi, an annually laminated lake from West Africa. We then examine the impact of this new age model on estimates of the timing of late glacial changes in the West African monsoon.

## 2. Materials and methods

### 2.1. Site description

Lake Bosumtwi is a small, meromictic lake in the tropical dry forest zone of southern Ghana (6° 30'N, 1° 25'W; Fig. 1). The lake fills a well-preserved meteorite impact crater that formed  $1.07 \pm 0.05$  Ma in Precambrian greenschist and intruding granite bedrock (Koeberl et al., 1998). The lake has a diameter of ca. 8 km and a depth of 75 m and is surrounded by steep crater walls, which reach an elevation of approximately 110 m above the modern lake surface. The catchment is internally draining and, based on studies of the modern lake hydrology, the lake is isolated from the surrounding regional groundwater table (Turner et al., 1996). As a result, the elevation of the lake within the crater is extremely sensitive to the balance between rainfall inputs to

the crater and evaporation from the lake surface (Shanahan et al., 2007a). The large depth to diameter ratio, combined with the sheltering of the lake to prevailing winds by the steep crater walls, minimizes seasonal mixing of the water column and helps to maintain deep water anoxia, resulting in the preservation of fine sediment laminations (Shanahan et al., 2008a).

The crater is heavily vegetated with lowland forest taxa and well-developed tropical soils. However, most of the flat, natural terraces and stream floodplains have been converted to agriculture (primarily maize, plantain or cassava). Steep exposures of paleolacustrine sediments are exposed in many riverbanks, where streams have dissected the softer sedimentary units. In the steeper portions of the crater these deposits have been eroded down to bedrock.

### 2.2. Sediment lithology and stratigraphy

During a series of site visits between 1999 and 2004, a set of 10 piston and gravity cores were collected from the central portion of the lake in order to construct a composite lithology for the upper ca. 10.9 m of the lake sediment record. The sediment–water interface for this lithologic section was retrieved using an extensive set of freeze and box cores which were able to preserve a record of fine, cm- to mm-scale laminations (Shanahan et al., 2008a). In 2004, a series of additional cores were collected during the Intercontinental Drilling Program (ICDP) sediment coring expedition to the lake, which successfully collected several complete sediment records spanning the entire 290 m sediment sequence to bedrock (Peck et al., 2005). This allowed us to extend the composite sediment record developed from the piston cores back to the analytical limit for radiocarbon dating (~50 kyr), which is the focus of this work. A description of lithologic and paleoclimatic

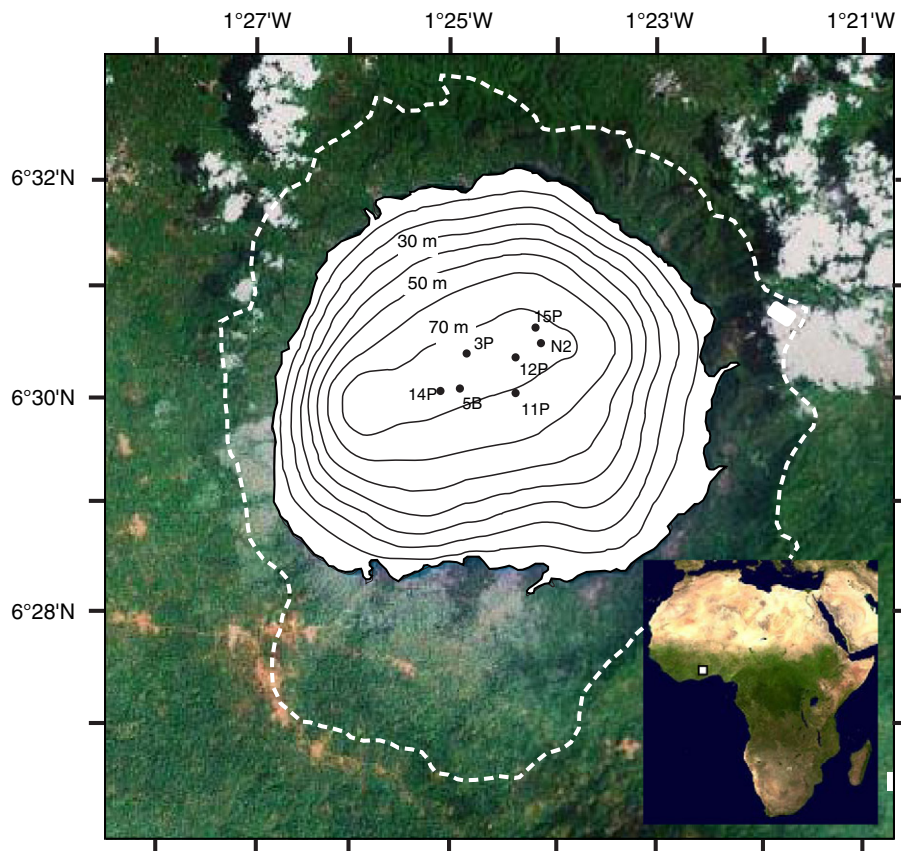


**Fig. 1.** Location of coring sites in Lake Bosumtwi, southern Ghana. Satellite image shows the location of the crater rim and the largely vegetated catchment area. Contours: lake bathymetry in meters below lake surface. Black circles indicate the location of cores which were used to generate the composite radiocarbon calibration. Inset: location of Lake Bosumtwi in the humid, lowland forest zone of West Africa.

changes over the remainder of the 1.07 Ma sediment record will be detailed elsewhere.

The sediments from Lake Bosumtwi display fine, cm- and mm-scale laminations over most of their length, with the exception of the interval between 2.1 and 3.9 m (standardized relative meter composite depth scale: RMCD), which is a lithologically massive, organic-rich unit containing abundant well-preserved remains of the cyanobacteria *Anabaena* (Unit S1).  $\delta^{15}\text{N}$  data for this interval are extremely depleted (0 to +2‰) consistent with the dominance of productivity by nitrogen-fixing cyanobacteria. Previous studies of this unit have interpreted it as reflecting a highly eutrophic, deep lacustrine system associated with extremely high and stable lake level, and possibly a reduction in rainfall seasonality (Talbot and Johannessen, 1992). This interpretation is consistent with the presence of lacustrine deposits on the crater walls as much as 100 m above the modern lake surface deposited during this time interval (Talbot and Delibrias, 1980; Shanahan et al., 2006).

Detailed studies of the fine laminations from the interval above unit S1 demonstrate that the mm-scale layers are annual in nature and derive from the seasonal input of terrigenous inorganic material to the lake during the summer monsoon season (Shanahan et al., 2007b). The nature of laminations deeper in the section has not been studied in detail to assess whether they are annual, but their visual and geochemical characteristics are similar to those near the surface, so it is probable that they are annual as well (Shanahan et al., 2007b). In addition to the mm-scale annual laminae, the sediments are also characterized by easily identifiable “marker” laminae, which are visually prominent either because they are thicker, or because they are distinctly different in color and composition (Fig. 2). In general, these visually prominent bands are either made up of Fe and Mn-rich carbonates, or are microturbidites (Shanahan et al., 2007b).

The marker bands are remarkably consistent across the central deep basin and provide a means for correlating between cores from different sites on cm scales. Although there are intervals where distinct marker bands are less apparent, intervals of consistently thicker or thinner mm-scale laminae appear much darker than the surrounding sediments in photographs and can provide additional markers that can be used to correlate between deepwater core sites (Fig. 2). In the upper 10 m of laminated sediments, there is no interval greater than ca.

20 cm without at least 1 well-defined marker band or visual tie point and overall, the frequency of marker bands is close to 5–10 cm. Visual matches are supported by correlations between downcore magnetic susceptibility profiles (Fig. 3). These correlations were used to generate a match between cores at different sites throughout the basin that is accurate to better than 10 cm, and allowed us to transfer radiocarbon dates from different cores onto a single depth profile (the relative meter composite depth scale - RMCD). This allows us to present a single composite radiocarbon chronology for the lake.

### 2.3. Geochronology

Several previous studies have sought to generate radiocarbon age models for Lake Bosumtwi in support of their sediment core-based paleoclimate studies (Talbot and Johannessen, 1992; Russell et al., 2003; Peck et al., 2004). The earliest work conducted by Talbot and Johannessen (1992) was based on 13 conventional radiocarbon ages on bulk organic material on two cores (B6 and B7 taken from the center of the lake). Subsequent radiocarbon dating of cores collected by Talbot (B6, B2) as well as on cores collected by Peck and coworkers (12P and 19P) targeted the transition between the *Anabaena*-rich unit (S1) and the uppermost laminations in order to better constrain the timing of late-Holocene drying (Russell et al., 2003). This involved radiocarbon dating a variety of materials including bulk organic matter, charcoal and pollen isolated from the sediments (Russell et al., 2003). Large amounts of scatter between radiocarbon ages collected at the same depth and a substantial (~1000 yr) age reversal associated with the transition to laminated sediments made it impossible to place a firm age estimate on the timing of the transition. However, radiocarbon ages on bulk material deeper in the unit S1, away from this lithological transition were more stratigraphically consistent and were used to produce a linearly extrapolated age estimate of  $3200 \pm 100$  cal yr B.P. (calendar years before present) for the onset of laminae formation and lake stratification.

Peck and coworkers generated an age model for piston cores collected in 2001 using an additional 30 AMS radiocarbon dates on bulk organic material and charcoal from cores 12P, 15P and 19P, and correlated the dates to a single standardized depth scale using magnetic susceptibility profiles (Peck et al., 2004). Several depth intervals between 400 and

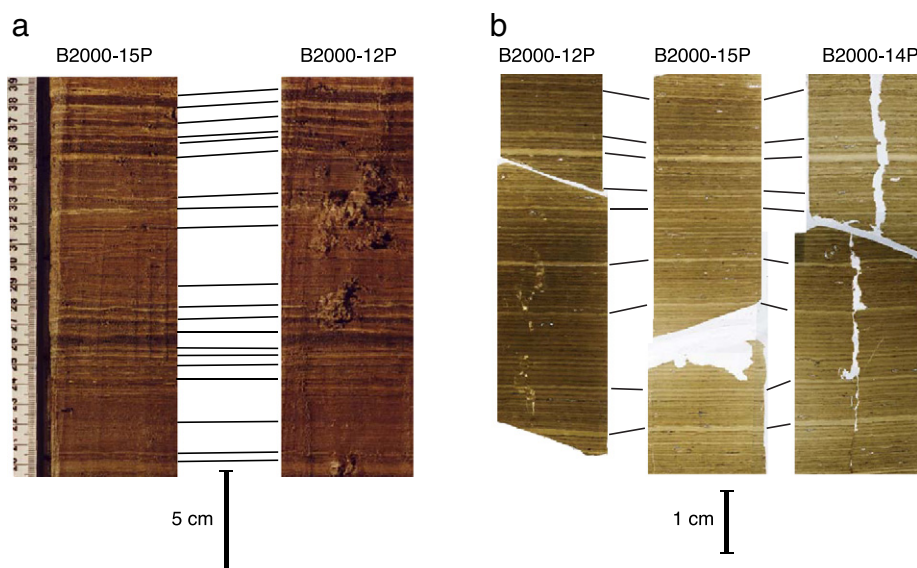


**Fig. 2.** Visual lamination matches between sediment cores from Lake Bosumtwi. a. Matches between macro-scale marker laminae in photographs of piston core 15P and 12P. Correlations can be made to <10 cm over most of the core lengths using marker laminae in photographs. b. Laminae-scale matches are also evident in transmitted light photographs of sediment thin sections from cores 12P, 15P and 14P. Correlations between marker bands in thin sections allow cm-scale correlations. However, correlations at sub-mm scales using individual laminae are also possible.

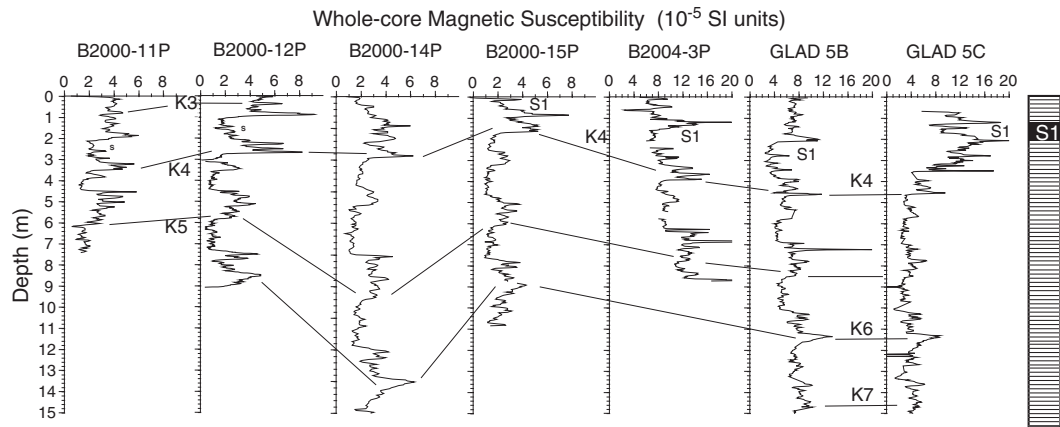


**Fig. 3.** Correlations between piston and drill cores. Solid lines and labels indicate major tie points. Correlations are based upon whole-core magnetic susceptibility. Right: generalized stratigraphy. Most of the core is laminated except section S1, which is massive and organic rich.

800 cm depth (e.g., 15–20 ka on their age model) displayed significant scatter and necessitated the removal of outliers. The resultant age-depth model was based upon linear interpolation over intervals where the ages were relatively reliable, and by linear regression over intervals where the scatter was large and identification of outliers was difficult (Peck et al., 2004). Using this age model, Peck and coworkers noted that the timing of distinct peaks in magnetics (attributed to greigite formation) occurred synchronously with North Atlantic Heinrich events, consistent with climate model-based predictions of a weaker West African monsoon circulation during intervals of significantly reduced Atlantic meridional overturning circulation (Peck et al., 2004). However, as is typical in classical age modeling, no attempt was made to quantify age model uncertainties or their potential impact on the assessment of synchronicity between the MS events and North Atlantic climate variability.

Most recently, Shanahan and coworkers produced a new high-resolution age model for the uppermost laminated unit (above unit S1) (Shanahan et al., 2009). Laminae counts,  $^{210}\text{Pb}$  dating and identification of the  $^{14}\text{C}$  “bomb-pulse” were all in agreement to within 1–3 yr over the last century, providing strong support for the annual nature of laminae. Although radiocarbon dates on bulk organic matter from above unit S1 were anomalous, collagen from articulated fish skeletons at three depths yielded radiocarbon dates consistent with varve counts, supporting the use of laminae counts to develop an age model down to the base of this unit (Shanahan et al., 2008a). Based on laminae counting, the transition from the organic rich, Anabaena unit (S1) to finely laminated sediments occurred at 2660 cal. yr BP (Shanahan et al., 2009). While it is difficult to estimate the true uncertainties in the laminae counts, previous studies have suggested that laminae counts in varved lake systems can underestimate the age by as much as 10% as a result of undercounting (Hajdas et al., 1995; Brauer et al., 2000; Hajdas and Bonani, 2000; Tian et al., 2005) (~266 yr). Even using this conservative laminae count error, the laminae count and radiocarbon age estimates are significantly different for this stratigraphic transition.

#### 2.4. Radiocarbon dating

To develop a more robust age model extending back to the limit of radiocarbon (i.e. ~50 kyr), we radiocarbon dated 125 samples in addition to the existing samples previously measured by Russell et al. (2003) and the radiocarbon dates on the collagen of articulated fish bone skeletons previously reported (Shanahan et al., 2008a). Dates reported previously for cores 19P and B2 and B6 were not used because of difficulties in correlating these cores at laminae scales. Plant macrofossils were scarce throughout the sediment record, which necessitated

the use of bulk organic matter for dating. However, in core sections spanning the last glacial maximum charred grass material was particularly abundant and samples of this material were hand-picked from 1 cm<sup>3</sup> samples for radiocarbon dating. To do so, bulk sediment samples were freeze dried and the grass charcoal was either picked individually with forceps or floated out using Type 1, ultrapure water. These macrofossil samples were typically small ( $\mu = 0.316$  mg). Bulk organic material from similar depths as the charcoal samples was also dated for comparison.

The majority of the samples were subjected to standard Acid-Alkali-Acid (AAA) pretreatment to remove dissolved humic acids prior to combustion and graphitization (Mook and Streurman, 1983). However, a subset of samples from the deepest sections of the core was pretreated using Acid-base-Oxidation (ABOX) pretreatment (Bird et al., 1999). The ABOX pretreatment method is a more aggressive chemical treatment designed to remove more of the secondary carbon, while leaving the primary indigenous elemental carbon behind. In addition, a subset of samples from near the base of the studied section was combusted and graphitized on a low-blank vacuum line (Bird et al., 1999; Pigati et al., 2007). The low blank line was specifically developed for reducing the uncertainties associated with contamination blanks when measuring samples near the limit of the radiocarbon dating method and has the potential to extend the limit of the radiocarbon dating method (Pigati et al., 2007). Following pretreatment and graphitization, all samples were submitted to the University of Arizona Accelerator Mass Spectrometry Facility for AMS radiocarbon dating. Radiocarbon ages were calibrated using the IntCAL09 calibration curve (Reimer et al., 2009) and are reported as the mean and 2- $\sigma$  standard deviation (Supplementary Table 1). Calibrated ages are plotted in Fig. 4 as the normalized 2- $\sigma$  calibrated age distribution, as computed using the OXCAL software (Bronk Ramsey, 2001).

#### 2.5. Laminae counting

Previous studies of laminated sediments from above unit S1 demonstrated that they are annual in nature (Shanahan et al., 2008a). This work used a combination of laminae counts,  $^{210}\text{Pb}$  dating, identification of the mid-20th century thermonuclear “bomb-pulse” and natural radiocarbon dating to confirm the varve chronology. In the present study, we followed procedures for identifying, counting and measuring laminae that are similar to those used earlier. At least three overlapping cores were used for analysis at all depths (from a combination of: drill core GLAD04-5B and piston cores BOS-3P, 14P, 12P, 15P). Laminae analyses were performed entirely on epoxy-resin embedded sediment thin sections because previous work had demonstrated the difficulty in identifying fine laminae directly from sediment core photographs. Laminae counts and thickness measurements were performed by

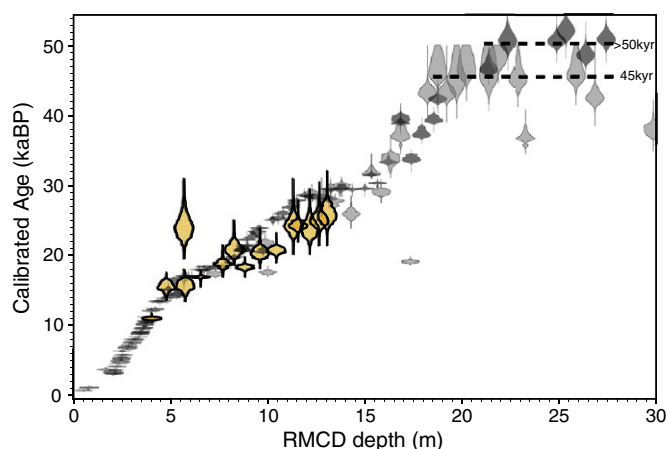


**Fig. 4.** The complete radiocarbon dataset from Lake Bosumtwi from piston cores PC-3, 12P, 15P, 14P and the GLAD800 drill core 5B. Cores were correlated using laminae matches and magnetic susceptibility and are plotted on a standardized (RMCD) depth scale. Radiocarbon dates were calibrated using the OXCAL software program and the Intcal09 radiocarbon calibration curve and are plotted as probability distributions. Light grey samples were pretreated by Acid-base-Acid (ABA) and combusted and graphitized on a standard vacuum extraction line. Yellow samples (dark outlines) were prepared in the same manner but had small sample sizes or poor graphitization yields. Dark grey samples were pretreated by ABA but were combusted and graphitized on a specialized low radiocarbon blank vacuum line. Labeled dashed lines highlight the differences in the age at which radiocarbon dates plateau using the traditional (~45 kyr) and low-blank (>50 kyr) radiocarbon lines. Note that dates plotted as >50 kyr were not calibrated because they exceeded the age limit of the Intcal09 calibration curve.

matching thin section scale marker laminae between overlapping cores, and then where possible, matching individual laminae between these marker bands across cores. Thickness measurements were based on a minimum of 3 measurements per laminae, avoiding areas with evidence for sediment disturbance or deformation. The laminae based chronology was only completed to a depth of ~10 m, because we lacked overlapping cores from multiple sites with which to construct the chronology below that depth (though this could be done in the future with cores from additional GLAD04 drill sites).

Unlike laminae counts at the top of the core, which can be counted back sequentially from the surface (i.e. if the core was collected in 2005, then the most recent lamina should be 2005), laminae counts on sediments below the unlaminated Anabaena-rich unit S1 are “floating.” To place the laminae counts on an absolute age scale, we employ a Monte Carlo-based radiocarbon “wiggles matching” approach (Bronk Ramsey et al., 2001). This approach seeks to find the optimal match between the uncalibrated radiocarbon dates from the Lake Bosumtwi composite sediment record and the Intcal09 radiocarbon calibration curve. To do so, it uses laminae counts as a constraint on the time elapsed between individual dated samples from the sediment cores and varies the amount of time (i.e., laminae) missing in the interval between the base of the Anabaena-rich section and the surface. An optimal fit is selected based upon a chi-squared minimization of the difference between the Intcal09 reference  $^{14}\text{C}$  curve and the uncalibrated dates from the sediment core.

A challenge in taking this approach is addressing the uncertainties in the radiocarbon calibration curve, the uncalibrated sediment core  $^{14}\text{C}$  ages and the potential errors in laminae counting (which are expected to increase downcore). In the approach used here, Monte Carlo methods are utilized to address the potential influence of these uncertainties on the model fit. The optimal fit is determined from a large number of iterations (i.e., >10,000) during which estimates of uncalibrated  $^{14}\text{C}$  ages from the Intcal09 radiocarbon calibration curve and the sediment core samples are randomly generated from their means and standard deviations assuming that the errors are distributed normally. To account for the potential influence of increasing errors in laminae counts, we assume a constant 10% error in the counts, which

is probably reasonable based on estimates in the literature (Hajdas et al., 1995; Brauer et al., 2000; Hajdas and Bonani, 2000; Tian et al., 2005). Because this approach makes the error in the laminae counts proportional to the total counts, it results in a wider margin of uncertainty and greater flexibility in the model fit in the lower portion of the record.

## 2.6. Age modeling

Traditionally, age–depth models for sediment records have been generated via relatively simple and straightforward approaches such as linear interpolation or fitting of a simple spline curve through the calibrated radiocarbon ages (Blaauw, 2010). However, these approaches ignore the fact that calibrated ages cannot be accurately represented by a single age because the calibration typically generates ages with irregular distributions. Furthermore, most studies provide no estimate of the errors associated with model based age estimates and can potentially lead to biased or incorrect chronologies (Blaauw, 2010). Recently, several studies have highlighted the potential problems associated with neglecting age model errors and recommended that more robust age modeling approaches need to be utilized particularly when examining high frequency limnological changes in sediment archives (Heegaard et al., 2005; Bronk Ramsey, 2008; Blaauw, 2010). One approach (“classical age modeling”) is to generate calibrated age distributions for each radiocarbon-dated sample and to use Monte Carlo methods to produce a series of potential age models by randomly selecting from these distributions. The optimal age–depth model is then computed from the weighted mean of all Monte Carlo iterations (Blaauw, 2010). However, this method of age modeling generally produces large age–depth uncertainties and has difficulty addressing issues associated with outliers. An alternative approach utilizes Bayesian techniques for calibration and age modeling simultaneously. The use of Bayesian techniques differs from “classical” models in that prior information such as stratigraphic ordering is incorporated into the calibration approach (Buck et al., 1991). In other words, calibrated age distributions and age models should be consistent with the fact that the samples occur in a particular sequence, and that the ages themselves should increase with depth. Based on this approach, the methods also provide some means of assessing the viability of the model and the presence of outliers (Bronk Ramsey, 2008; Blaauw and Christen, 2011). These techniques have been shown to produce reliable age–depth models, with more realistic estimates of age model uncertainties than “classical” approaches (Blockley et al., 2007, 2008; Bronk Ramsey, 2008).

In the present study, we generate an age model for the Lake Bosumtwi sediment record using Bayesian approaches, as implemented in the freely available R software package BACON (Blaauw and Christen, 2011) and using the IntCal09 radiocarbon calibration curve (Reimer et al., 2009). In calibrating ages and developing an age–depth model, BACON assumes that the data are in stratigraphic order and models the sediment accumulation rates as a function of depth using a simple gamma autoregressive process. By modeling accumulation rates, the model avoids the use of simple smoothing algorithms and prevents unrealistic changes in sedimentation rates when interpolating between ages. Posterior distributions needed for Bayesian analysis are generated using the “t-walk,” a self adjusting Markov Chain Monte Carlo algorithm (Christen and Fox, 2010), which has the advantage that it does not require tuning and is less parameterized than other Bayesian models (e.g., OXCAL, BChron). Radiocarbon ages are determined using the methodology of Christen and Perez (Christen and E, 2009), which is based on the generalized robust Student-t model, rather than the more common Normal model. Identification of outliers is performed using the “shift outlier” approach of (Christen, 1994) and (Blaauw and Christen, 2005), which has been shown to be robust to the presence of outliers.

Incorporation of the laminae counts in the upper two-meter laminated section of the age–depth model (above unit S1) is problematic

for several reasons. Using all of the individual laminae counts as ages in the model (e.g., 2660 individual ages) is probably incorrect because the laminae counts are not independent and this would place too much weight on the varve ages in the age-depth model. Alternatively, if we incorporate only the estimate of the age of the base of the laminated unit in the model ( $2660 \pm 130$  cal yr B.P.; assuming a  $\pm 5\%$  error in laminae counts) as a tie point in our age depth model, the model misses the exponential decrease in sedimentation rate that is evident in laminae thickness measurements. Furthermore, because this approach represents the laminae counts as a single age, whereas there are multiple radiocarbon ages, the radiocarbon dates are more heavily weighted in age modeling, and the laminae counts have a weak influence on the model. As a compromise in our age model approach, we incorporate one varve count tie point every 100 yr over the upper  $2660 \pm 130$  cal yr B.P., which is close to the radiocarbon dating resolution. This approach allows us to include the laminae counts and the information they provide about the changes in sedimentation over the upper 2 m in the age model without weighting these ages too heavily. The influence of this approach on our results is discussed in more detail in Section 4.1.

Bayesian age-depth modeling assumed a gamma distribution (shape = 2) for sedimentation rates with a mean of  $20 \text{ yr cm}^{-1}$ , based on laminae thickness measurements. The model included the prior condition that the surface was  $-50 \pm 0$  cal yr B.P.

### 3. Results

#### 3.1. Radiocarbon age anomalies

Calibrated radiocarbon ages from Lake Bosumtwi show significant spread with depth, indicative of problems with radiocarbon contamination (Fig. 4). The amount of scatter and inconsistencies between dates from the same or adjacent depths also appears to increase with depth and, in particular, appears to be much larger in the early part of the record, prior to the Holocene. Some of this scatter is likely the result of the remobilization of old organic matter from the lake margins, particularly during severe lake regressions when old organic matter is eroded from the catchment and transported to the lake basin. Previous work on the uppermost part of the sediment record showed that this effect was particularly severe following the rapid lake level decline in the mid-Holocene, causing age anomalies as large as 3 kyr (Shanahan et al., 2008a). Though the size of these anomalies decreases towards the sediment water interface, anomalies as large as several hundred years are still evident at 300 cal yr B.P., ~2.5 kyr after the initial decline in lake level and hundreds of years after the lake level minima at ~1 kyr BP. Anomalous dates seem to show significant scatter, regardless of the material dated (Russell et al., 2003) and age reversals are common, most likely reflecting the episodic transport of aged carbon during turbidity flows. Furthermore, modern waters from Lake Bosumtwi yield  $^{14}\text{C}$  values that are similar to atmospheric  $\text{CO}_2$ , and collagen from articulated fish bones found at depth yield radiocarbon ages that are in agreement with laminae counts, suggesting that age anomalies are not due to lake “reservoir” effects (Shanahan et al., 2008a).

#### 3.2. Dating of grass cuticle charcoal

In an attempt to address potential problems associated with the dating of bulk organic carbon, we isolated samples of grass cuticle charcoal at select intervals during the glacial for radiocarbon dating, as this material is fragile and presumably less likely to be reworked (Peck et al., 2004). However,  $\text{CO}_2$  yields for the charcoal were generally low (e.g., 60–80%), which we interpret as the result of significant amounts of phytolith silica being present in the combusted material. Because of the low  $\text{CO}_2$  and subsequent graphite yields, count rates for this material were low and radiocarbon ages on charcoal had

larger uncertainties than dates for bulk organic matter. A comparison of bulk and grass charcoal ages suggests that the dates on grass charcoal ages tend to yield ages that are younger than the corresponding bulk ages, though the differences vary widely (e.g., from 0 to 3000 yr; Fig. 5).

There are two potential explanations for the radiocarbon age discrepancies. The first is that the charcoal dates are younger because they are too fragile to be preserved during reworking and therefore, when preserved, they are unlikely to be reworked and provide the most reliable ages. While the offsets between grass charcoal and bulk OM are larger and more variable than seen elsewhere (Blaauw et al., 2011), they are generally consistent with this interpretation; where they differ, grass charcoal ages are almost always younger than the bulk ages.

An alternate possibility is that the grass charcoal dates are anomalously young because of preferential contamination with young carbon. While this was not our original expectation, there are several reasons to believe this to be the case. First, our observation has been that very small samples combusted and graphitized on a conventional sample processing line produce anomalous ages that are biased young and should be treated with caution. Presumably this is because of the inclusion of very small amounts of modern  $\text{CO}_2$  contamination, which are nevertheless significant because of the small relative amounts of  $\text{CO}_2$  produced from the samples. Second, a subset of bulk samples pretreated using the ABOX pretreatment method, meant to leave behind only primary indigenous graphitic material like charcoal, yielded ages that were more consistent with the bulk dates, and older than grass charcoal dates from similar depths. Furthermore, with few exceptions the bulk dates are internally consistent, even when combining dates from multiple cores using magnetic susceptibility and laminae-based matches, whereas the grass dates show poor agreement with one another across correlated cores. Such consistency between the bulk dates from cores

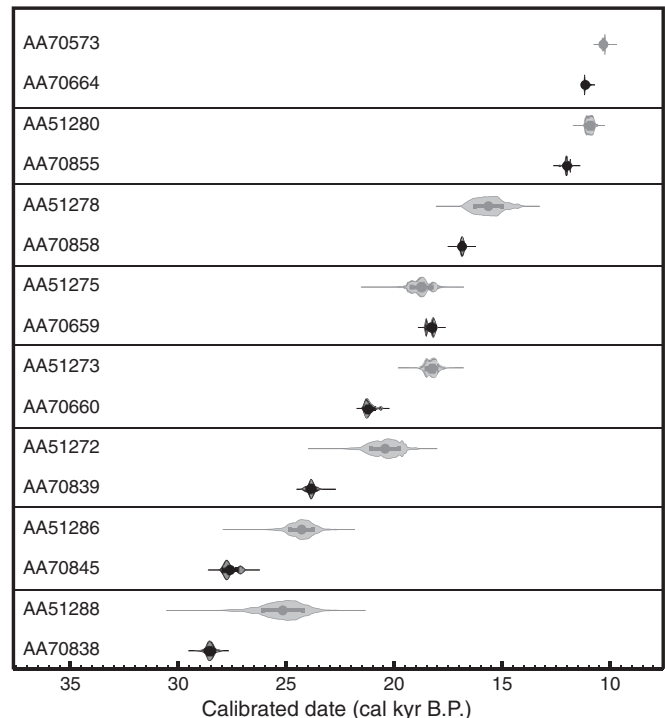


Fig. 5. Comparison between calibrated radiocarbon dates on bulk organic matter (black) and charcoal (grey) from either identical or similar depths in the lake Bosumtwi sediment core record. Calibrated age distributions are based on individual age calculations using the program OXCAL and reflect errors in the AMS age determinations and variations in the calibration curve. Note that in all cases, the grass charcoal ages are the same or younger than the ages on bulk material, though the large errors in charcoal ages make these differences statistically insignificant in most cases.

across the deep basin and at different depths is unlikely if they were significantly influenced by the transport of aged carbon to the basin. We would expect that the factors influencing erosion, transport and drifting of old carbon to differ from location to location causing the degree of contamination to differ, leading to offsets in bulk dates from the same depth at different sites. This is not what we observe. Finally, a comparison of radiocarbon ages with laminae counts based on radiocarbon “wobble matching” (see below) supports the validity of the bulk organic matter dates in age model development.

The observation that the dates are systematically younger than the bulk dates suggests the incorporation of young CO<sub>2</sub> into the samples. If we assume a modern <sup>14</sup>C content for the contamination (FM<sub>m</sub> = 1), then we can compute the amount of CO<sub>2</sub> contamination (C<sub>m</sub>) required to produce the observed differences between dates using the following mass balance equation:

$$C_m = C_{\text{sample}} \times \frac{FM_{\text{sample}} - FM_{\text{true}}}{FM_m - FM_{\text{true}}}$$

Based on a comparison of grass charcoal and bulk organic samples from the same or very similar depths, the amount of modern carbon contamination was less than ~5% (2–7 µg C).

There are two potential explanations for this amount of modern carbon contamination in the grass charcoal samples. The most obvious explanation is that during combustion or graphitization of small samples, small leaks in the vacuum line contaminated the samples with small amounts of atmospheric CO<sub>2</sub>. However, while very small samples can yield anomalous dates, the size of the leaks needed to produce the observed age offsets are unlikely, as one would expect then to also be evident in line blanks which are run frequently (and which are typically closer to 2 µg C). An alternative explanation is that the age anomalies are associated with modern CO<sub>2</sub> adsorbed to the silica phytolith material contained in the grass charcoal samples. While this potential complication has not, to our knowledge, been previously identified in dating of grass charcoal, this has been suggested as the cause of anomalously young radiocarbon ages for diatom opal (Zheng et al., 2002). In this earlier study, modern contamination blanks on radiocarbon-dead diatomaceous opal samples from the southern ocean yielded ages of 15.3–33.1 kyr, which is equivalent to 15–130 µg of modern carbon contamination. In the same study, the inclusion of glass wool in the sample combustion line increased blanks from 2 to 15 µg of carbon, supporting the hypothesis that the modern contamination was derived from CO<sub>2</sub> adsorption onto silica. Estimates of modern carbon contamination in the grass charcoal samples are well within this range for potential contamination with adsorbed CO<sub>2</sub>, suggesting that this is a viable mechanism for explaining the anomalously young ages for this material.

### 3.3. Traditional versus low-blank radiocarbon dating

An additional source of scatter in the radiocarbon data comes from samples collected from > 18 m depth (RMCD depth scale). All samples below this depth that were prepared using a traditional radiocarbon vacuum extraction line yield ages that are essentially indistinguishable from one another (e.g., 40–45 kyr). This is significantly below the practical radiocarbon dating limit of 55 kyr and, like the charcoal dates, suggests that there may be issues with contamination of small amounts of modern <sup>14</sup>CO<sub>2</sub>. With the goal of extending our radiocarbon-based age model to at least 50 kyr, we prepared an additional set of overlapping samples with a more rigorous pretreatment procedure (ABOX) (Bird et al., 1999) and combusted and graphitized the samples on a specially designed low-blank radiocarbon vacuum line at the University of Arizona (Pigati et al., 2007). The resultant data extend the chronology significantly with depth (to > 22 m), though the absolute datable age limit is limited to 47–50 kyr because of the limits of the IntCal09 radiocarbon calibration curve (Reimer et al., 2009). Because these samples were pretreated differently and combusted and graphitized using

different vacuum lines, it is unclear whether the improved resolution from the second dataset is due to improved sample processing line blanks, or rather is linked to something about the properties of the organic material that survives AAA versus ABOX pretreatment. Regardless, the data suggest that dating of lake sediment samples near the analytical limit of radiocarbon can be improved using these techniques. In order to take advantage of these additional low-blank dates in our age depth modeling we exclude all samples measured with a traditional extraction line below the depth where the ages appear to plateau (ca. 18 m). The result allows us to extend our radiocarbon age model by 4 m and ca. 10 kyr (Fig. 4). However, because of a lack of standardized calibration for samples beyond the limit of the IntCal09 calibration curve, all samples older than 45 <sup>14</sup>C kyr were also excluded from age-depth modeling at this time.

### 3.4. Age-depth modeling

Our final radiocarbon dataset, omitting these biased samples, is shown in Fig. 6. In general, the dates are internally consistent, with a few (*n* = 15) obvious outliers that are stratigraphically out of order by several hundred to thousands of years. Some proportion of anomalous dates is expected from any scenario, and the number of visually apparent outliers is not particularly anomalous in comparison with what has been reported in other studies (e.g., 20%). A number of approaches have been proposed to deal with outliers in datasets like this, though it has been argued that the best approach remains visual identification because most require an assumed expectation of some number of anomalous dates (Blaauw and Christen, 2005; Blaauw et al., 2007; Bronk Ramsey, 2008). In the Lake Bosumtwi dataset, in addition to the obvious outliers, there are a significant number of samples that are inconsistent by only a few decades to centuries. While these inconsistencies would probably not be apparent in most radiocarbon datasets because of the low radiocarbon sample density, because of the large number of closely spaced dates in this study, accentuates these small offsets, and it is problematic to evaluate which dates are outliers. Similarly, attempts to use methods of automated outlier detection, like the one implemented in the program OXCAL, are unsuccessful because the model also lacks sufficient a priori information to make unbiased choices about outlier selection.

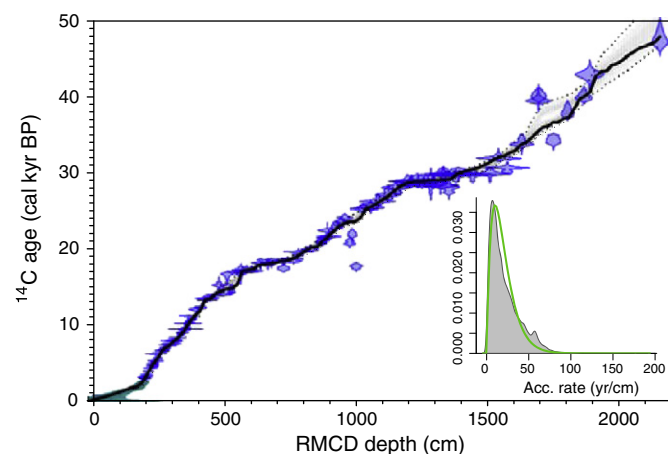


**Fig. 6.** Age-depth model for Lake Bosumtwi based on calibrated radiocarbon ages computed using the Bayesian age modeling software BACON (Blaauw et al., 2011). Blue dots represent the 2-σ calibrated age estimates for individual radiocarbon ages. The black line represents the computed age depth curve. The dashed lines represent the Monte-Carlo based estimates of the age-depth model uncertainties. Dates on grass charcoal material and on older samples not prepared on the low-blank graphitization line were excluded and are not shown here, as discussed in the text. Inset: a comparison of modeled (green curve) and calculated sediment accumulation rate distributions. The model was run with 20 sections, and a 20 yr/cm mean accumulation rate.

Because we had no unbiased way of selecting outliers, we opted to include all dates in our age model except the aforementioned grass charcoal and high blank samples from > 18 m depth. The age modeling approach used here in BACON has been shown to be very robust to the presence of outliers (Christen, 1994; Blaauw and Christen, 2005) in radiocarbon age modeling. Uncertainties in the age–depth model are in the range of several hundreds of years (Fig. 6) and encompass the small reversals between adjacent dates, while at the same time ignoring visually obvious outliers. However, because the age model uses a Bayesian approach that takes into account the stratigraphic ordering of the data, as well as the radiocarbon age error distributions, it produces an age–depth model with smaller uncertainties than those generated by classical age–depth modeling (e.g., CLAM; Blaauw, 2010). 95% confidence intervals are smallest during the Holocene ( $205 \pm 160$  yr), increase slightly during the glacial ( $360 \pm 120$  yr) and are largest at the base of the record ( $1660 \pm 160$  yr), due to a combination of decreasing sample density, larger calibration uncertainties and increases in scatter.

### 3.5. Comparison of $^{14}\text{C}$ ages and laminae counts

Support for the radiocarbon age model is provided by a comparison with the record of laminations. To do so, laminae counts were placed on an annual chronology by wiggle matching uncalibrated radiocarbon dates against the Intcal09 calibration curve, while holding fixed the number of laminae (years) between each date. Using this approach, the optimal match for the top of the laminated unit is  $12,777 \pm 838$  cal. yr BP. Visual comparison of the laminae age model against the calibrated radiocarbon data provides support for the annual nature of the laminations (Fig. 7). The laminae age–depth curve reproduces several of the inflection points in the radiocarbon curve, including the inflection points at 450, 700 and 1150 cm depth. However, offsets between the two curves do occur and indicate that some of the laminations may be undercounted. For example, there is a clear divergence between the laminae count age model and the radiocarbon age model in the interval below 1100 cm depth. These differences suggest that some laminations were missed over this interval.

A direct comparison of calibrated radiocarbon ages and laminae counts yields a slope of  $1.085 \pm 0.0277$  ( $r^2 = 0.97$ ), indicating a mean discrepancy of 8.5% for the full interval of overlap (Fig. 7). The observation that the slope of this relationship is steeper than the 1:1 line supports the visual observation that the laminae may have been undercounted over some intervals in the record. This discrepancy is comparable to that seen in age models developed from other laminated records such as Steel Lake (Tian et al., 2005), Lake Meerfelder Maar (Brauer et al., 2000) and Lake Holzmaar (Hajdas et al., 1995; Hajdas and Bonani, 2000). Unlike in these records, however, it is unclear where the differences in the Lake Bosumtwi chronologies originate, as there are several discrete intervals where the slope of the  $^{14}\text{C}$ –varve relationship is locally steeper than the 1:1 line, suggesting local errors in lamination counts that are larger than 8.5%. As pointed out by Blaauw et al. (2011) in their work on Lake Challa, errors in their age model increase significantly after 12,550 cal yr B.P., which they suggest could be due in part to errors in the IntCal09 calibration curve, and some of these offsets could be local in nature. An alternate possibility is that the local offsets may be due to changes in the character or nature of the laminae, which results in inaccurate layer counts over these intervals. While this is certainly possible, over the interval between 16 and 18 ka, where there is a significant offset from the 1:1 line between varve counts and radiocarbon ages, we see little visual evidence of a major difference in laminae other than their thicknesses. In the future, more work may be necessary to resolve the origin of these differences and their impact on the development of high-resolution sediment laminae chronologies.

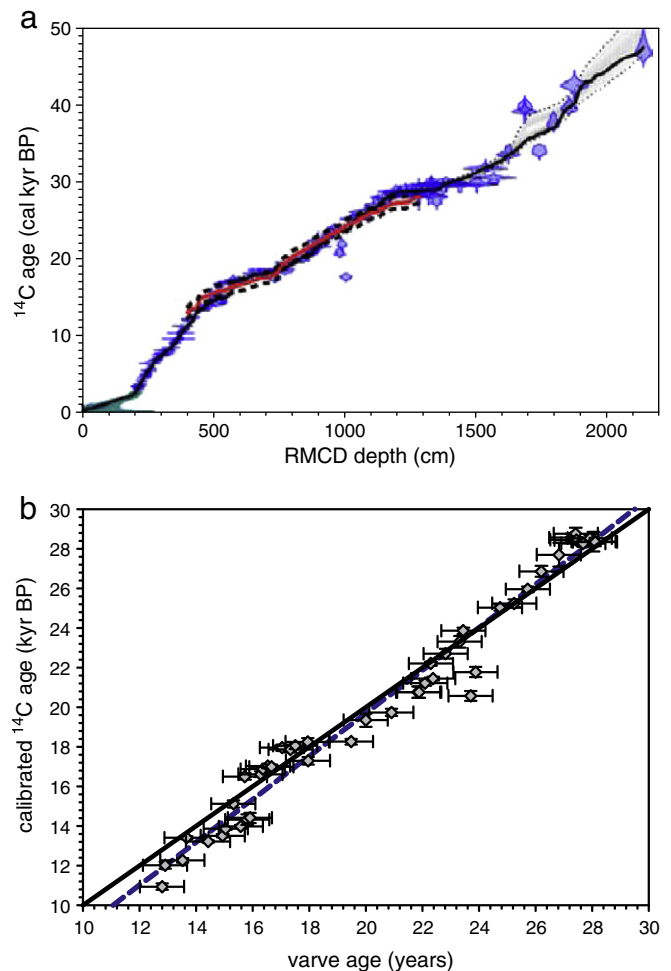


Fig. 7. Comparison of varve and radiocarbon chronologies. a. Same as Fig. 6. Solid red line shows composite laminae counts as a function of depth. The depth of these counts is fixed based upon matching of the varve chronology to the core photographs using marker bands. The match in age (y-axis) was made by radiocarbon “wiggle-matching.” Dashed lines represent  $2\sigma$  errors in the wiggle-match. b. Comparison between calibrated radiocarbon ages and optimized wiggle-match varve ages. The solid line represents a 1:1 match; the dashed line shows a best fit linear regression to the data.

## 4. Late Quaternary changes in sedimentation rate and climate at Lake Bosumtwi

### 4.1. The end of the Holocene African Humid Period (AHP)

During the early Holocene, much of equatorial and north Africa was much wetter than today, as a result of increased northern hemisphere summer insolation, which resulted in an intensification of the North African monsoon (Kutzbach and Guetter, 1986; Kutzbach and Liu, 1997). The African Humid Period (AHP) ended during the mid-to late-Holocene as summer insolation declined, resulting in one of the most significant and widespread climatic changes of the last 10,000 yr in tropical Africa (e.g., Gasse and Campo, 1994; Hoelzmann et al., 1998; Jolly et al., 1998; deMenocal et al., 2000; Gasse, 2000, 2002; Lezine, 2009). At Lake Bosumtwi, the end of the AHP is evident in both paleolake highstand data (Talbot and Delibrias, 1980; Shanahan et al., 2008b) and sediment cores (Talbot and Johannessen, 1992; Russell et al., 2003). In sediment cores, mid-Holocene drying manifests itself as a distinct lithologic transition from massive, black, organic-rich muds (unit S1) to finely laminated sediments (Talbot and Johannessen, 1992; Russell et al., 2003). This

transition is also apparent in  $\delta^{15}\text{N}$  data, which shows an abrupt shift of +4‰ across this boundary, interpreted to reflect a shift from a deep, well-mixed eutrophic lake a shallower, stratified meromictic system similar to today (Talbot and Johannessen, 1992). Previous estimates for the age of this boundary from linear interpolation of radiocarbon dates ( $3200 \pm 100$  cal yr B.P.; (Russell et al., 2003) and laminae counting ( $2660 \pm 130$  varve yr BP; (Shanahan et al., 2008a)) differ significantly.

The Bayesian age-depth modeling approach offers a means of estimating the age of this lithological transition by allowing us to combine both the radiocarbon ages and the laminae counts and their uncertainties in age-depth modeling. Based upon our age-depth model, the best estimate of the age of this boundary is  $2880 \pm 100$  cal yr B.P. (Fig. 8, a and b). This age is sensitive to the estimates of errors in laminae counts (which are assumed to be  $\pm 5\%$ ) and the number of laminae count tie points used in the model (here we use incorporate one laminae count age every 100 yr over the upper 2 m in order to capture the structure of sedimentation rate changes). Changes in these parameters can shift the age of the boundary by ca. 100–200 yr. Regardless, our chronology suggests that the end of the AHP at Lake Bosumtwi occurred several thousands of years after the abrupt drying at 5500–4500 cal yr B.P. recorded in sites from North Africa (deMenocal et al., 2000; Gasse, 2000). However, it is consistent with palynological evidence for a significant loss of primary forest between ~3000 and 2200 cal yr B.P. in records from a number of sites in Cameroon, the Central African Republic, Gabon and Congo (Maley, 1991; Elenga et al., 1994; Maley and Brenac, 1998; Vincens et al., 1999; Sowunmi, 2002; Schefuss et al., 2005; Ngomanda et al., 2009). The visual abruptness of the transition from unit S1 to the uppermost laminated sediments at Lake Bosumtwi is striking, and suggests that hydrological changes were extremely abrupt, occurring in just a few years. Most other records indicate that late Holocene drying, though relatively abrupt, took at least 500–1000 yr, and may have even started as early as 4000 cal yr B.P., with an increase in intensity after ca. 3000 cal yr B.P. (Vincens et al., 1999). Visual inspection of sediment thin sections across this transition indicates that regular laminations do appear abruptly at the top of unit S1. However, irregularly spaced microturbidites appear as much as 5–10 cm below the top of unit S1, indicating that at least some significant hydrological changes occurred before the dramatic onset of laminations at the top of unit S1. Furthermore, lamination thicknesses, major element abundances and oxygen isotope ratios of authigenic carbonates all change gradually between the S1 boundary and ~1000 cal yr B.P., indicating progressively drier conditions throughout the late Holocene (Shanahan et al., 2009). Together these data suggest that this visually abrupt sedimentological transition may

represent a threshold response to gradually decreasing lake level and hydrology rather than an abrupt climate change.

The data from Bosumtwi and at other sites in Atlantic equatorial Africa indicate that the West African monsoon weakened more gradually and much later in the humid, equatorial tropics of West Africa than at higher latitudes, but that it was synchronous over much of the Guinea coastal region, spanning both hemispheres. The fact that these changes occur both more gradually and later than at higher latitudes suggests that changes in the monsoon circulation over the Holocene were decoupled between the high and low latitudes, perhaps reflecting differences in their relative sensitivities to nonlinear land surface feedbacks on monsoon rainfall. The delayed mid- to late-Holocene climate transition in Atlantic equatorial Africa has previously been attributed to either a large-scale atmospheric reorganization (Russell et al., 2003; Shanahan et al., 2008b) or a shift to a more seasonally arid climate as the northward limit of the monsoon retreated southward over the mid- to late-Holocene (Maley, 1997). More detailed and continuous reconstructions of the evolution of the AHP in equatorial Africa, from Lake Bosumtwi and elsewhere are needed to better understand the mechanisms behind these changes and their apparent synchrony.

#### 4.2. Millennial-scale variability in sedimentation rate and climate

The radiocarbon age-depth model for Lake Bosumtwi shows several significant plateaus, with the most significant of these at ~16–19 kyr and 29–31 kyr and a smaller plateau at 24 kyr (Fig. 6). Though such plateaus in calibrated age-depth curves can reflect plateaus in the radiocarbon calibration curve, in the present case these events are too large to be caused by changes in the residence time of  $^{14}\text{C}$  in the atmosphere. Instead, we attribute them to episodic increases in the delivery of sediment from the crater margins to the central basin (Fig. 9). However, cores and thin sections are laminated over these intervals, indicating that the high rates of deposition are not the result of mass flow events. Furthermore, terrigenous laminae thicknesses increase substantially over these intervals, suggesting that these changes in sedimentation rate reflect increases in the seasonal erosion and transport of sediments to the deep basin (Fig. 9).

Increased erosion rates during these intervals could be the result of either more intense or more seasonal precipitation, leading to higher sediment loads in tributary streams within the crater, or due to lowered lake level caused by decreased precipitation that exposed unvegetated crater slopes and made the central coring sites effectively closer to the tributary inputs. Multiple lines of independent evidence support the latter hypothesis. First, during the late Holocene (>3 kyr), when lake levels were low, there is a significant increase in sedimentation rates,

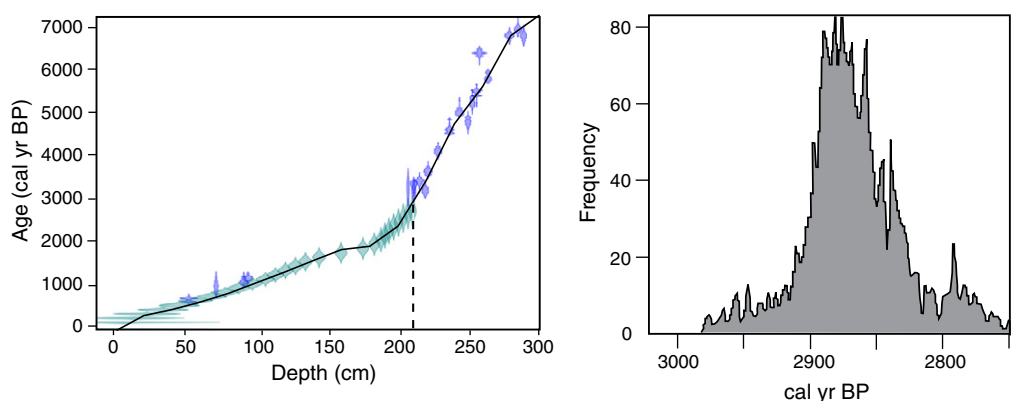


**Fig. 8.** Age model estimate for the end of the African Humid Period (AHP) at Lake Bosumtwi. a. Age modeling results. The black line represents the computed age depth curve, blue symbols represent the calibrated age estimates for individual radiocarbon ages and the green symbols represent the laminae count tie points used in the age model. The dashed line is the depth of the abrupt transition from unlaminated to laminated sediments associated with the end of the AHP (210 cm). b. Frequency distribution of Bayesian age-depth model estimates from the AHP transition.

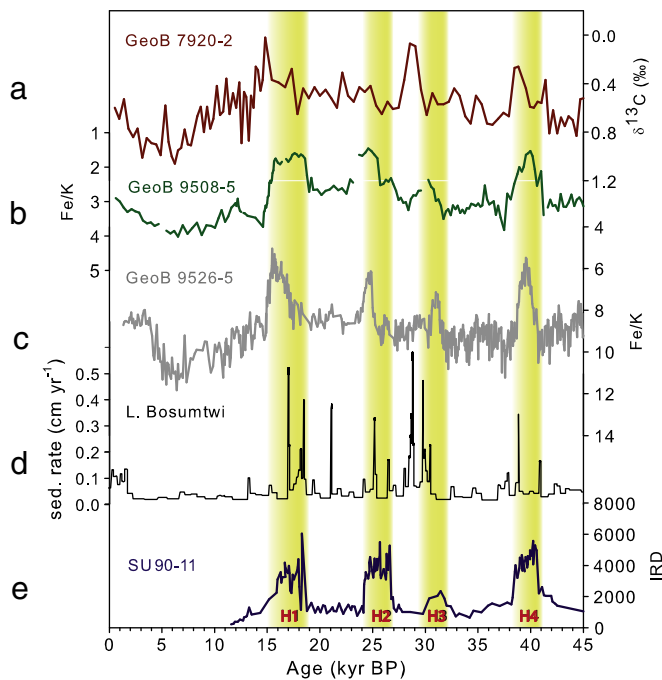


**Fig. 9.** West African paleoclimate records displaying millennial-scale variability (a–d) compared against ice rafted debris (IRD) from the North Atlantic (e) (Jullien et al., 2007). Vertical bars highlight approximate timing of Heinrich events (H1–H4) based on intervals of enhanced IRD concentrations. a.  $\delta^{13}\text{C}$  of *C. wuellerstorfi* as a proxy of wind driven productivity from marine core GeoB7920 (20°45.09' N, 18°34.9' W; Tjallingii et al., 2008). b and c. Fe/K ratios as a proxy for terrigenous runoff in marine core GeoB 9508 (15°29.9' N, 17°56.88' W; Mulitza et al., 2008) and GeoB 9526 (12°26' N, 18°03' W; Zariess et al., 2011). d. Changes in sedimentation rate computed for Lake Bosumtwi, Ghana (this study). e. Changes in ice rafted debris (IRD) concentrations in core SU90-11 (Jullien et al., 2007).

consistent with increased delivery of sediments to the basin (Talbot and Delibrias, 1980; Russell et al., 2003; Shanahan et al., 2008b). Furthermore, during the preceding interval (~10–5 cal kyr), when the lake was overflowing, sedimentation rates are at their lowest rates of the last 50 kyr BP. Similarly, submerged beaches dated to ~16.3 kyr indicate that lake level had dropped by more than 60 m at that time (Brooks et al., 2005; Peck et al., 2005; Shanahan et al., 2008b), consistent with increased sedimentation rates between ~16–19 kyr (Fig. 9). Thickness measurements on annual laminations from the uppermost portion of the sediment record spanning the instrumental record indicate that this sedimentation rate-climate relationship also holds on decadal timescales, with thicker laminae occurring during periods of anomalously dry conditions (Shanahan et al., 2007b). These data strongly suggest that the crater morphology of Lake Bosumtwi imparts a sedimentation rate response that is most strongly controlled by variations in the size of the erodible catchment associated with changes in lake level, and not the intensity of precipitation. For this reason, we hypothesize that the intervals with high sedimentation rates apparent in the age-depth model are the result of millennial-scale intervals with anomalously dry conditions and enhanced sediment deposition.

The evidence for millennial-scale droughts during the last glacial at Lake Bosumtwi is consistent with proxy evidence from other sites in West Africa (Fig. 9). Published results from Atlantic marine cores off the northwest African margin and West African lake sediment records show dramatic increases in dust flux, upwelling driven productivity and decreases in sea surface temperatures (SSTs), which have been interpreted previously as reflecting a southward migration of the mean annual position of the Intertropical Convergence Zone (ITCZ), the monsoon trough and/or a strengthening of the dry northeast trade winds (Street-Perrott and Perrott, 1990; Adegbe et al., 2003; Mulitza et al., 2008; Itambi et al., 2009; Niedermeyer et al., 2010; Zariess and

Mackensen, 2010; Zariess et al., 2011). Though the timing and relative magnitudes of these events differ slightly, within their chronological uncertainties they are broadly synchronous. Together, they suggest that most of the North African monsoon region was impacted by millennial-scale droughts.

Previous studies have attributed these millennial-scale droughts to a southward shift in the mean position of the ITCZ in response to reductions in the strength of the Atlantic Meridional Overturning Circulation (AMOC) and changes in Atlantic SST gradients during North Atlantic Heinrich events (Street-Perrott and Perrott, 1990; Mulitza and Ruhlmann, 2000; Dahl et al., 2005). The broadly similar timing of intervals of ice rafted debris (IRD) deposition in the North Atlantic during Heinrich events (Bond and Lotti, 1995; Jullien et al., 2007) and West African droughts supports this mechanism. At the same time, freshwater hosing experiments with coupled ocean–atmosphere climate models designed to simulate changes in circulation associated with discharges of freshwater into the North Atlantic also produced drought over much of West Africa, primarily through southward shifts in the location of the ITCZ or the monsoon trough (Dahl et al., 2005). The record from Lake Bosumtwi suggests that these events extended to at least 6°N. This finding is inconsistent with models simulating a simple ITCZ-like response because an equatorial contraction of the ITCZ results in increased precipitation near the equator, including the region around Bosumtwi (Shanahan et al., 2008b). More recent simulations of Heinrich-type slowdowns of the AMOC using the NCAR Climate System Model CCSM2.0.1 produced more widespread drought in response to these events that is more consistent with proxy data, including that from Lake Bosumtwi (Mulitza et al., 2008). They indicate that southward shifts in the ITCZ during AMOC slowdowns are accompanied by intensified moisture export in the African Easterly Jet, which reduces the amount of available moisture for precipitation over coastal West Africa. A similar argument was also made recently on the basis of a compilation of records spanning Heinrich event 1 throughout the Asian and African monsoon region (Stager et al., 2011). Stager and colleagues argued that the large spatial extent of Heinrich 1 drought requires a change in the intensity and moisture content of the tropical rainbelt, and cannot be explained simply through a southward shift in its mean position. The Lake Bosumtwi data supports these findings, and indicates that similar spatially extensive droughts occurred in association with earlier Heinrich ice rafting events.

Age model uncertainties for both records of West African drought and IRD deposition in the North Atlantic preclude an absolute determination of the phasing of these events, though the broad similarity in timing of multiple events during the last glacial suggests they are linked. Similarly, the magnitudes and durations of the millennial-scale droughts differ widely between proxy records and should be interpreted with caution because they may reflect differences in depositional conditions, proxy response and resolution as much as differences in paleoclimatic conditions. For example, the absence of a correlative drought in the Lake Bosumtwi record with events seen in other West African proxy reconstructions during the time of Heinrich event 4 is likely a consequence of the lower resolution age model during this interval rather than a difference in the climate response of these regions during this event. More work needs to be done to assess the nature of these differences in order to better understand how the West African monsoon responds to changes in the AMOC.

## 5. Conclusions

In this study, high-resolution AMS radiocarbon dating was used to generate a chronology for the last ~45 kyr of sedimentation at Lake Bosumtwi, Ghana, a crucial archive of past climate change, in equatorial West Africa. The high resolution dating approach provided several key age modeling insights that would not have been evident with typical, low resolution dating approaches. First, dating of terrestrial macrofossils was found to be problematic, as the small sample sizes resulted in

large uncertainties, substantially larger scatter and a bias towards younger ages.  $^{14}\text{C}$  dates on bulk organic matter less than 35 kyr in age were much more internally consistent and deemed more reliable, despite previous evidence to the contrary. Beyond ~35 kyr, reliable ages were only possible with more rigorous sample pretreatment techniques and the use of a specialized low blank extraction and graphitization lines. Comparison of lamination counts and radiocarbon age modeling yields similar results, supporting previous suggestions that laminations produced during the last glacial are annual in nature.

The resultant age-depth model displays several age plateaus, which are attributed to increased sedimentation rates during intervals of decreased precipitation (Figs. 6 and 9). Though age model uncertainties and changes in sampling resolution downcore preclude an absolute determination of the synchrony and relative magnitudes of millennial-scale droughts across West Africa, and their association with changes in the AMOC, the visual similarities between the records suggest that they are linked. If correct, the results from Lake Bosumtwi indicate that drought conditions extended southward to the West Africa coast, and require not only changes in the seasonal migration of the tropical rainbelt but also changes in moisture availability or intensity of convection.

Supplementary data to this article can be found online at <http://dx.doi.org/10.1016/j.palaeo.2012.08.001>.

## Acknowledgements

We thank the people of Abono, Ghana and the other towns surrounding Lake Bosumtwi for their assistance during fieldwork as well as the researchers in the Arizona AMS Facility for their help in preparing and analyzing radiocarbon samples. The research was funded in part by National Science Foundation grants EAR0601998, ATM0401908, ATM0214525, and ATM0096232.

## References

- Adegbie, A., Schneider, R., Rohl, U., Wefer, G., 2003. Glacial millennial-scale fluctuations in central African precipitation recorded in terrigenous sediment supply and freshwater signals offshore Cameroon. *Palaeogeography, Palaeoclimatology, Palaeoecology* 197 (3), 323–333.
- Bird, M.I., et al., 1999. Radiocarbon dating of "old" charcoal using a wet oxidation, stepped-combustion procedure. *Radiocarbon* 41 (2), 127–140.
- Blaauw, M., 2010. Methods and code for 'classical' age-modelling of radiocarbon sequences. *Quaternary Geochronology* 5 (5), 512–518.
- Blaauw, M., Christen, J., 2005. Radiocarbon peat chronologies and environmental change. *Journal of the Royal Statistical Society: Series C: Applied Statistics* 54, 805–816.
- Blaauw, M., Christen, J., 2011. Flexible paleoclimate age-depth models using an autoregressive gamma process. *Bayesian Analysis* 6 (3), 457–474.
- Blaauw, M., Bakker, R., Andres Christen, J., Hall, V.A., van der Plicht, J., 2007. A Bayesian framework for age modeling of radiocarbon-dated peat deposits: case studies from the Netherlands. *Radiocarbon* 49 (2), 357–367.
- Blaauw, M., et al., 2011. High-resolution  $^{14}\text{C}$  dating of a 25,000-year lake-sediment record from equatorial East Africa. *Quaternary Science Reviews* 30, 3043–3059.
- Blockley, S.P.E., Blaauw, M., Ramsey, C.B., van der Plicht, J., 2007. Building and testing age models for radiocarbon dates in Lateglacial and Early Holocene sediments. *Quaternary Science Reviews* 26 (15–16), 1915–1926.
- Blockley, S., Ramsey, C., Lane, C., Lotter, A., 2008. Improved age modelling approaches as exemplified by the revised chronology for the Central European varved lake Soppensee. *Quaternary Science Reviews* 27 (1–2), 61–71.
- Bond, G.C., Lotti, R., 1995. Iceberg discharges into the North Atlantic on millennial time scales during the last glaciation. *Science* 267, 1005–1010.
- Brauer, A., Endres, C., Zolitschka, B., Negendank, J., 2000. AMS radiocarbon and varve chronology form the annually laminated sediment record of Lake Meerfelder Maar, Germany. *Radiocarbon* 42 (3), 355–368.
- Bronk Ramsey, C., 1998. Probability and dating. *Radiocarbon* 40 (1), 461–474.
- Bronk Ramsey, C., 2001. Development of the radiocarbon calibration program. *Radiocarbon* 43 (2A), 355–363.
- Bronk Ramsey, C., 2008. Deposition models for chronological records. *Quaternary Science Reviews* 27 (1–2), 42–60.
- Bronk Ramsey, C., van der Plicht, J., Weninger, B., 2001. 'Wiggle matching' radiocarbon dates. *Radiocarbon* 43 (2A), 381–389.
- Brooks, K., et al., 2005. Late-Quaternary lowstands of lake Bosumtwi, Ghana: evidence from high-resolution seismic-reflection and sediment-core data. *Palaeogeography Palaeoclimatology Palaeoecology* 216 (3–4), 235–249.
- Buck, C., Kenworthy, J., Litton, C., Smith, A., 1991. Combining archaeological and radiocarbon information: a Bayesian approach to calibration. *Antiquity* 65, 808–821.
- Buck, C., Christen, J., James, G., 1999. BCal: an on-line Bayesian radiocarbon calibration tool. *Internet Archaeology* 7 [http://interarch.ac.uk/journal/issue7/buck\\_toc.html](http://interarch.ac.uk/journal/issue7/buck_toc.html).
- Christen, J., 1994. Summarizing a set of radiocarbon determinations: a robust approach. *Applied Statistics* 43 (3), 489–503.
- Christen, J.A., E.S.P., 2009. A new robust statistical model for radiocarbon data. *Radiocarbon* 51 (3), 1047–1059.
- Christen, J., Fox, C., 2010. A general purpose sampling algorithm for continuous distributions (the t-walk). *Bayesian Analysis* 4 (2), 263–282.
- Dahl, K.A., Broccoli, A.J., Stouffer, R.J., 2005. Assessing the role of North Atlantic freshwater forcing in millennial scale climate variability: a tropical Atlantic perspective. *Climate Dynamics* 24, 325–346.
- deMenocal, P., Ortiz, Joseph, Guilderson, Tom, Sarnthein, Michael, 2000. Coherent High- and Low-Latitude Climate Variability During the Holocene Warm Period. *Science* 288, 2198–2202.
- Elonga, H., Schwartzt, D., Vincens, A., 1994. Pollen evidence of Late Quaternary vegetation and inferred climate changes in the Congo. *Palaeogeography, Palaeoclimatology, Palaeoecology* 109, 345–356.
- Gasse, F., 2000. Hydrological changes in the African tropics since the Last Glacial Maximum. *Quaternary Science Reviews* 19, 189–211.
- Gasse, F., 2002. Diatom-inferred salinity and carbonate oxygen isotopes in Holocene waterbodies of the western Sahara and Sahel (Africa). *Quaternary Science Reviews* 21 (7), 737–767.
- Gasse, F., Campo, E.V., 1994. Abrupt post-glacial climate events in West Asia and North Africa monsoon domains. *Earth and Planetary Science Letters* 126, 435–456.
- Hajdas, I., Bonani, G., 2000. Radiocarbon dating of varve chronologies: Sopensee and Holzmae Lakes after ten years. *Radiocarbon* 42, 349–353.
- Hajdas, I., et al., 1995. AMS radiocarbon dating for annually laminated sediments from Lake Holzmaar, Germany. *Quaternary Science Reviews* 14, 137–143.
- Heegaard, E., Birks, H., Telford, R., 2005. Relationships between calibrated ages and depth in stratigraphical sequences: an estimation procedure by mixed-effect regression. *The Holocene* 15 (4), 612–618.
- Hoelzmann, P., et al., 1998. Mid-Holocene land-surface conditions in northern Africa and the Arabian peninsula: a data set for the analysis of biogeophysical feedbacks in the climate system. *Global Biogeochemical Cycles* 12 (1), 35–51.
- Itambi, A.C., Von Dobeneck, T., Multza, S., Bickert, T., Heslop, D., 2009. Millennial-scale northwest African droughts related to Heinrich events and Dansgaard-Oeschger cycles: evidence in marine sediments from offshore Senegal. *Paleoceanography* 24 (1), PA1205.
- Jolly, D., Harrison, S.P., Damnati, B., Bonnefille, R., 1998. Simulated climate and biomes of Africa during the late quaternary: comparison with pollen and lake status data. *Quaternary Science Reviews* 17 (6–7), 629–657.
- Jullien, E., et al., 2007. Low-latitude "dusty events" vs. high-latitude "icy Heinrich events". *Quaternary Research* 68 (3), 379–386.
- Koeberl, C., Reimold, W.U., Blum, J.D., Chamberlain, C.P., 1998. Petrology and geochemistry of target rocks from the Bosumtwi impact structure, Ghana and comparison with Ivory Coast tektites. *Geochimica et Cosmochimica Acta* 62 (12), 2179–2196.
- Kutzbach, J.E., Guetter, P.J., 1986. The influence of changing orbital parameters and surface boundary conditions on climate simulations for the past 18,000 years. *Journal of the Atmospheric Sciences* 43 (16), 1726–1759.
- Kutzbach, J.E., Liu, Z., 1997. Response of the African Monsoon to orbital forcing and ocean feedbacks in the Middle Holocene. *Science* 278, 440–443.
- Lezine, A.M., 2009. Timing of vegetation changes at the end of the Holocene Humid Period in desert areas at the northern edge of the Atlantic and Indian monsoon systems. *Comptes Rendus Geoscience* 341 (8–9), 750–759.
- Maley, J., 1991. The African Rain Forest vegetation and paleoenvironments during the late Quaternary. *Climatic Change* 19, 79–98.
- Maley, J., 1997. Middle to late holocene changes in tropical Africa and other continents: Paleomonsoon and sea surface temperatures. In: Dalfes, G.K.H.N., Weiss, H. (Eds.), *Third Millennium BC Climate Change and Old World Collapse: NATO ASI Series*. Springer-Verlag, Heidelberg, pp. 611–640.
- Maley, J., Brenac, P., 1998. Vegetation dynamics, paleoenvironments and climatic changes in the forests of western Cameroon during the last 28,000 years BP. *Review of Palaeobotany and Palynology* 99 (2), 157–187.
- Mook, W., Streuerman, H., 1983. Physical and chemical aspects of radiocarbon dating, Strasbourg.
- Multza, S., Ruhlmann, C., 2000. African monsoonal precipitation modulated by Interhemispheric temperature gradients. *Quaternary Research* 53, 270–274.
- Multza, S., et al., 2008. Sahel megadroughts triggered by glacial slowdowns of Atlantic meridional overturning. *Paleoceanography* 23 (4), PA4206.
- Ngomanda, A., Neumann, K., Schweizer, A., Maley, J., 2009. Seasonality change and the third millennium BP rainforest crisis in southern Cameroon (Central Africa). *Quaternary Research* 71 (3), 307–318.
- Niedermeyer, E.M., et al., 2010. Orbital- and millennial-scale changes in the hydrologic cycle and vegetation in the western African Sahel: insights from individual plant wax  $\delta\text{D}$  and  $\delta^{13}\text{C}$ . *Quaternary Science Reviews* 29 (23–24), 2996–3005.
- Peck, J.A., et al., 2004. A magnetic mineral record of Late Quaternary tropical climate variability from Lake Bosumtwi, Ghana. *Palaeogeography Palaeoclimatology Palaeoecology* 215 (1–2), 37–57.
- Peck, J.A., et al., 2005. The Lake Bosumtwi Drilling Project: a 1Ma West African Paleoclimate Record. American Geophysical Union Fall Meeting, San Francisco.
- Pigati, J., Quade, J., Wilson, J., Jull, A., Lifton, N., 2007. Development of low-background vacuum extraction and graphitization systems for C-14 dating of old (40–60ka) samples. *Quaternary International* 166, 4–14.
- Reimer, P., et al., 2004. IntCal04 terrestrial radiocarbon age calibration, 0–26 cal kyr BP. *Radiocarbon* 46 (3), 1029–1058.

- Reimer, P.J., et al., 2009. INTCAL09 and MARINE09 radiocarbon age calibration curves, 0–50,000 Years cal BP. *Radiocarbon* 51 (4), 1111–1150.
- Russell, J., Talbot, M.R., Haskell, B.J., 2003. Mid-holocene climate change in Lake Bosumtwi, Ghana. *Quaternary Research* 60 (2), 133–141.
- Schefuss, E., Schouten, S., Schneider, R.R., 2005. Climatic controls on central African hydrology during the past 20,000 years. *Nature* 437 (7061), 1003–1006.
- Shanahan, T.M., et al., 2006. Paleoclimatic variations in West Africa from a record of late Pleistocene and Holocene lake level stands of Lake Bosumtwi, Ghana. *Palaeogeography Palaeoclimatology Palaeoecology* 242 (3–4), 287–302.
- Shanahan, T.M., Overpeck, J.T., Sharp, W.E., Scholz, C.A., Arko, J.A., 2007a. Simulating the response of a closed-basin lake to recent climate changes in tropical West Africa (Lake Bosumtwi, Ghana). *Hydrological Processes* 21 (13), 1678–1691.
- Shanahan, T.M., et al., 2007b. The formation of biogeochemical laminations in Lake Bosumtwi, Ghana and their usefulness as indicators of past environmental changes. *Journal of Paleolimnology* 40 (1), 339–355.
- Shanahan, T.M., et al., 2008a. The formation of biogeochemical laminations in Lake Bosumtwi, Ghana, and their usefulness as indicators of past environmental changes. *Journal of Paleolimnology* 40 (1), 339–355.
- Shanahan, T.M., et al., 2008b. Abrupt changes in the water balance of tropical West Africa during the late. *Quaternary Journal of Geophysical Research-Atmospheres* 113, D12107.
- Shanahan, T.M., et al., 2009. Atlantic Forcing of Persistent Drought in West Africa. *Science* 324 (5925), 377–380.
- Sowunmi, M.A., 2002. Environmental and human responses to climatic events in West and Central Africa during the late Holocene. In: Hassan, F.A. (Ed.), *Droughts, Food and Culture: Ecological Change and Food Security in Africa's Later Prehistory*. Kluwer, New York, pp. 95–104.
- Stager, J.C., Ryves, D.B., Chase, B.M., Pausata, F.S.R., 2011. Catastrophic drought in the Afro-Asian monsoon region during Heinrich event 1. *Science* 331 (6022), 1299–1302.
- Street-Perrott, F.A., Perrott, R.A., 1990. Abrupt climate fluctuations in the tropics: the influence of Atlantic Ocean circulation. *Nature* 343, 607–612.
- Talbot, M.R., Delibrias, G., 1980. A new late-Holocene water-level curve for Lake Bosumtwi, Ghana. *Earth and Planetary Science Letters* 47, 336–344.
- Talbot, M.R., Johannessen, T., 1992. A high resolution paleoclimatic record for the last 27,000 years in tropical West Africa from the carbon and nitrogen isotopic composition of lacustrine organic matter. *Earth and Planetary Science Letters* 110, 23–37.
- Telford, R., Heegaard, E., Birks, H., 2004a. All age–depth models are wrong: but how badly? *Quaternary Science Reviews* 23 (1–2), 1–5.
- Telford, R., Heegaard, E., Birks, H., 2004b. The intercept is a poor estimate of a calibrated radiocarbon age. *The Holocene* 14 (2), 296–298.
- Tian, J., Brown, T., Hu, F., 2005. Comparison of varve and  $^{14}\text{C}$  chronologies from Steel Lake, Minnesota, USA. *The Holocene* 15, 510–517.
- Tjallingii, R., et al., 2008. Coherent high- and low-latitude control of the northwest African hydrological balance. *Nature Geoscience* 1 (10), 670–675.
- Turner, B.F., Gardner, L.R., Sharp, W.E., 1996. The hydrology of Lake Bosumtwi, a climate-sensitive lake in Ghana, West Africa. *Journal of Hydrology* 183, 243–261.
- Vincens, A., et al., 1999. Forest response to climate changes in Atlantic Equatorial Africa during the last 4000 years BP and inheritance on the modern landscapes. *Journal of Biogeography* 26 (4), 879–885.
- Zarriess, M., Mackensen, A., 2010. The tropical rainbelt and productivity changes off northwest Africa: a 31,000-year high-resolution record. *Marine Micropaleontology* 76 (3–4), 76–91.
- Zarriess, M., et al., 2011. Bipolar seesaw in the northeastern tropical Atlantic during Heinrich stadials. *Geophysical Research Letters* 38, L04706.
- Zheng, Y., et al., 2002. Challenges in radiocarbon dating organic carbon in opal-rich marine sediments. *Radiocarbon* 44 (1), 123–136.